THE MEASUREMENT OF BACTERIAL TRANSLATION BY PHOTON CORRELATION SPECTROSCOPY

GREGORY B. STOCK, *Thomas C. Jenkins Department of Biophysics, The Johns Hopkins University, Baltimore, Maryland 21218 U.S.A.*

ABSTRACT Photon correlation spectroscopy is shown to be a practical technique for the accurate determination of translational speeds of bacteria. Though other attempts have been made to use light scattering as a probe of various aspects of bacterial motility, no other comprehensive studies to establish firmly the basic capabilities and limitations of the technique have been published. The intrinsic accuracy of the assay of translational speeds by photon correlation spectroscopy is investigated by analysis of synthetic autocorrelation data; consistently accurate estimates of the mean and second moment of the speed distribution can be calculated. Extensive analyses of experimental preparations of *Salmonella typhimurium* examine the possible sources of experimental difficulty with the assay. Cinematography confirms the bacterial speed estimates obtained by photon correlation techniques.

INTRODUCTION

Photon correlation spectroscopy (PCS) is a general technique for the detection and analysis of movement at a microscopic level. It has been applied to diverse problems ranging from the measurement of diffusion constants of macromolecules (7) to the detection of sarcomere motion in striated muscle (5). The first attempts to apply the technique to the analysis of bacterial motility were made in 1971 (10). Notwithstanding early optimism that this technique would soon be used routinely to assay bacterial motility, several complications in the interpretation of the photon correlation data first had to be overcome. Contributions due to translational movement had to be differentiated from those due to rotational movement. Detailed computations using several different models to describe bacterial scatterers (4, 14, 16) have clearly shown that contributions to the autocorrelation data from rotational movement are significant only at higher scattering angles. Low-angle data reflect only translational movement and are not distorted by rotational effects. These particular complications are not encountered with a related light scattering technique (13) that monitors the fluctuations in the number of particles in the scattering volume to obtain dynamical parameters. Unfortunately, other difficulties arise at the low bacterial concentrations required by this technique. Significantly, the longer time required for these measurements limits the range of problems that can be studied. The PCS studies treated in the present paper are all performed at bacterial densities high enough to avoid contributions from such fluctuations.

Another challenge has been to devise a satisfactory technique for extracting from the

autocorrelation data useful, accurate, and readily interpretable information about the speed distributions of the bacterial scatterers. Such a technique (17) is examined in detail in this paper.

Since 1972 a variety of papers have been published concerning the interpretation of photon correlation functions obtained from preparations of motile bacteria (8). For the most part these have consisted of rather detailed analyses of synthetic data generated with specific theoretical models, and have included little experimental data. When experimental results have been presented, they have not been thoroughly justified or accompanied by a complete discussion of the analyses employed (1, 11, 12). One problem has been that no verification, using an independent measuring technique, of the results obtained by PCS has been presented. Thus, doubts as to the validity of the PCS assay have persisted.

On the one hand, attempts have been made to use increasingly complex models of the the structure and motion of the bacterium (3, 6) to interpret the nontranslational components of the autocorrelation data. Unfortunately, because of the large number of descriptive parameters used, it is possible to mimic experimental data without severely constaining the various parameters. The difficulties in obtaining a unique and precise description of the motion stem from the fact that experimental preparations contain bacteria of a wide range of shapes exhibiting many different motions. Alteration of the distribution of values of any parameter will materially affect the autocorrelation data. Specific changes in different parameters can result in equivalent modifications of the data, and this precludes an accurate unique determination of the parameter distributions. Autocorrelation data taken from a large, heterogeneous population of bacteria allow only qualitative conclusions about the rotational parameters of the bacteria.

On the other hand, precise and detailed information about the translational speed distributions of a bacterial culture can be obtained from low-angle scattering data, which can be collected rapidly without significantly perturbing the culture. It is as an assay of translation that PCS should prove most useful for the study of bacterial motility. This paper is an attempt both to evaluate the limitations of the fitting technique—the method of splines— and to determine what information about the bacterial speed distribution can be obtained under actual experimental conditions. For PCS to be useful as a general assay, consistent results must be achievable under a variety of conditions; thus, the temptation to optimize experimental conditions for light scattering in ways that might restrict the usefulness of the assay has been avoided. The bacterial strain used in these studies possesses no unusual motile properties that would serve to simplify the motile assay. Moreover, the light-scattering results have been verified by comparison with independent cinematographic measurements of bacterial translation.

METHODS

All chemicals were reagent grade. Polystyrene latex spheres were obtained from Dow Chemical Co. (Midland, Mich.). The bacteria used, *Salmonella typhimurium*, strain SB3507 (trpB223), were obtained from the stocks of P. E. Hartman. Phosphate buffer (CHE) contained 0.1 mM EDTA and 10 mM K_2PO_4 (pH 7.0).

Permanent bacterial stocks were frozen in the presence of dimethyl sulfoxide and used every few weeks to grow temporary nutrient broth (NB) stocks. For each experiment, after a 10-fold dilution of an overnight culture, cells were freshly grown at 37°C with constant aeration. The cells were harvested in mid-log phase by centrifugation at 600 *g*. The pellet was gently washed and resuspended in either NB or CHE. Alternatively, the washed and still concentrated bacteria were stored at 4°C and added, immediately before data collection via intramedic tubing to the thermally preequilibrated medium in the scattering cuvette. Nonmotile bacteria were obtained by subjecting the bacteria to an acid wash at pH 1.5.

A detailed description of the experiment apparatus and alignment procedures has been given elsewhere (18). For low-angle measurements, special care had to be taken to avoid heterodyning from light scattered by the cuvette windows. By examining the scattered light by eye through the front aperture of the collection optics, the cuvette position could be adjusted to eliminate flare from the cuvette. The incident radiation, 632.8 nm, was unfocused. The bacteria were contained in a cuvette that was thermally regulated to prevent convection.

Cinematographic results were obtained with a variable film speed camera (165, Arriflex Co. of America, Woodside, N.Y.) and Kodak 3-x film (Eastman Kodak Co., Rochester, N.Y.). Bacteria were photographed at a film speed of 16 frames/s, under phase contrast with a 40× objective. Speeds of individual bacteria were determined by marking the coordinates of bacterial images from successive film frames projected onto a viewing screen (18). Reproducible projection and magnification was insured by a reticle image on each frame. Due to the thinness ($\sim 8\ \mu m$) of the fluid layer between the microscope slide and cover slip, virtually all movement was within the focal plane. Nevertheless, only bacteria that remained in focus for at least 20 frames were included in the speed estimate. This further reduced any inaccuracies that might have resulted from the inability of such cinematography to measure velocity components perpendicular to the focal plane. Errors from this source are at most a few percent and would tend to cause an underestimation of bacterial speeds. The difficulties inherent in the cinematographic assay have been discussed at greater length elsewhere (18).

In fitting experimental autocorrelation functions, data were weighted in proportion to the standard deviations of the noise associated with the individual data points. Estimates of this noise were made by repeatedly collecting autocorrelation functions from single bacterial preparations and calculating the variances of the data points. An advantage of this method is that it emphasizes those regions of the autocorrelation function which are most invariant and reproducible from experiment to experiment. Thus, the motile parameters extracted closely reflect the characteristics of the experimental sample. The synthetic data were fitted in the same way; the noise at the individual data points was, however, computer-generated.

THEORETICAL BACKGROUND

At low scattering angles (<15°), the contribution to the autocorrelation data resulting from nontranslational motion of the bacteria can be neglected (16), and thus the expression (10):

$$g^{(1)}(\tau) = \int_0^\infty (\sin q\tau v/q\tau v)\, P(v)\, dv, \qquad (1)$$

where $g^{(1)}(\tau)$ is the field autocorrelation function, $P(v)$ is the particle speed distribution, and q is the magnitude of the scattering vector, becomes a valid approximation. Actually, the expression must be slightly modified to account for the concomitant diffusion of the actively translating bacteria. Also, computation is more straightforward if an additional term, β, is introduced to represent the fraction of bacteria that are nonmotile. Thus (17),

$$g^{(1)}(\tau) = e^{-D_T q^2 \tau}\left[\beta + (1 - \beta)\int_0^\infty (\sin q\tau v/q\tau v)\, P(v)\, dv\right], \quad (2)$$

where D_T is the diffusion constant of the bacteria and can be measured with nonmotile organisms.

A technique, the method of splines, was developed to extract $P(v)$ from the autocorrelation data (9, 17). It has several advantages: first, the integrals encountered are numerically tractable without requiring a rigid analytic form, unjustified by theory, to describe the bacterial speed distribution. Second, information about the speed distribution available from other sources can be advantageously incorporated into the fitting procedure. Finally, other techniques for $P(v)$ extraction are flawed: direct Fourier sine transformation of $g^{(1)}(\tau)$ is troubled by serious truncation problems, and the extraction of even speed moments directly from $g^{(1)}(\tau)$ is more subject to error and offers less readily interpretable information about the structure of $P(v)$ than does the spline technique (18). Actual measurements are of the intensity autocorrelation function, which is then normalized and labeled $g^{(2)}(\tau)$. A simple equation,

$$g^{(2)}(\tau) = 1 + |g^{(1)}(\tau)|^2, \quad (3)$$

relates the two functions. Here $g^{(1)}(\tau)$ is also normalized.

In a spline fit, the speed distribution function is represented as a linear combination of linearly independent polynomial basis functions. The coefficients of the combination are treated as parameters in a least-squares fitting procedure that selects those coefficients producing an autocorrelation function that best approximates the experimental data. These coefficients are then used to calculate a corresponding speed distribution that *ipso facto* best represents the autocorrelation data. This speed distribution is necessarily a piecewise polynomial, i.e., composed of smooth polynomial segments connected at junction points, denoted "knots." The form of the distribution depends upon the degree of the spline fit; for linear spline fits, it is simply a series of connected straight-line segments. The location of the knots are fixed before fitting and the values of the function at the knots are optimized by the fit (18).

RESULTS

Synthetic Data

Ideally, the speed distribution determined by spline fitting would be highly sensitive to changes in the autocorrelation function and highly insensitive to the details of the fitting procedure. If the number or the locations of the knots selected were to affect significantly the final distribution obtained, the utility of the technique would be seriously reduced. Both to consider these possibilities and to ascertain how much detail about the speed distribution could be determined from autocorrelation data, synthetic data were generated and analyzed. In this way, intrinsic limitations of the analytic technique could be examined in isolation, insulated from possible results of deficiencies in the experimental data or inadequacies in the theoretical model of bacterial motion. With synthetic data, the shape of the speed distribution function could

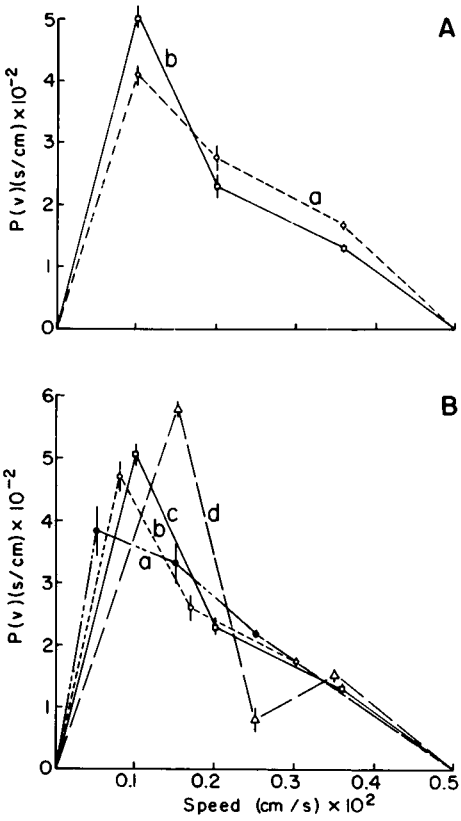

FIGURE 1

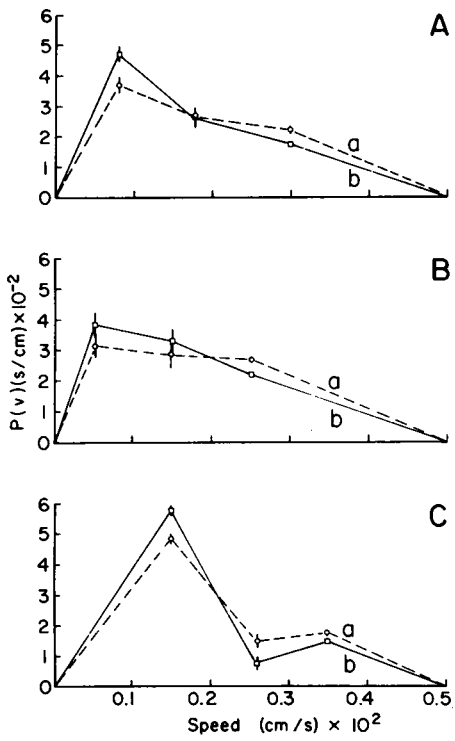

FIGURE 2

FIGURE 1 Sensitivity of the spline fits to knot position. (A) Two different speed distribution functions (——— and -----), whose moments are tabulated in Table I, were used to generate synthetic 60-point autocorrelation functions. For each of the distribution functions, 10 such autocorrelation functions with noise were generated and individually fitted with a spline function having knots at 0, 0.001, 0.002, 0.0036, and 0.005 cm/s. The mean and standard deviation of the mean for both sets of 10 fitted speed distributions are indicated (□, ◇) at each knot; they closely approximate the original distributions. (B) The 10 autocorrelation functions generated from distribution *b* were each fitted successively with four different knot sets. *a*. (0, 0.005, 0.0015, 0.0025, 0.005 cm/s); *b*. (0, 0.0008, 0.0017, 0.003, 0.005 cm/s); *c*. (0, 0.001, 0.002, 0.0036, 0.005 cm/s); and *d*. (0, 0.0015, 0.0025, 0.0035, 0.005 cm/s). For each knot set, the mean and standard deviation of the mean for the 10 fits are plotted.

FIGURE 2 Accuracy of the mean speed determination. For three different knot sets—A: (0, 0.0008, 0.0017, 0.003, 0.005 cm/s); B: (0, 0.0005, 0.0015, 0.0025, 0.005 cm/s); and C: (0, 0.0015, 0.0025, 0.0035, 0.005 cm/s)—the autocorrelation functions generated from the two speed distributions of Fig. 1 A (*a*, *b*) were fitted. For each knot set, the two fitted speed distributions, labeled *a* and *b*, are plotted. In each case, distribution *a* is displaced towards higher speeds.

be controlled, the amount of noise in the data could be varied, and the final fitted speed distribution function could be compared to the assumed speed distribution used to generate the data, with noise.

In these synthetic data experiments, an assumed speed distribution function was used to calculate the autocorrelation function, $g^{(2)}(\tau)$, that it would produce. This autocorrelation function was modified by the addition of independent random noise to the individual points, and then was fitted with a particular spline basis set. Finally, the fitted speed distribution function was compared to the original speed distribution function that had been assumed. This comparison verified the speed distribution extracted from the autocorrelation data, and was essential in evaluating the utility of the technique. The quality of the fit to the autocorrelation data was judged on another basis—the magnitude of the chi squared per degree of freedom, χ_ν^2. The noise added to each individual point of $g^{(2)}(\tau)$ was normally distributed, with zero mean, and, unless otherwise indicated, had a standard deviation of 1% of the value of $g^{(2)}(\tau)$ at each τ. The least-squares fits to $g^{(2)}(\tau)$ had a χ_ν^2 equal to 1 within error.

NUMBER OF BASIS SPLINE FUNCTIONS By examining several different speed distribution functions, each without discontinuities or sharp peaks and each zero at speeds greater than 50 μm/s, the number of spline basis functions needed to fit autocorrelation data adequately was determined. The generated autocorrelation data were fitted with a progressively decreasing number of spline basis functions until the quality of the fits, as indicated by the magnitude χ_ν^2, began to deteriorate. For the distributions considered, four basis elements were always sufficient to obtain a χ_ν equal to 1 within experimental error, three were usually so, and two were never so. This remained the case even when the noise level was reduced to 0.1%. Clearly, if so few basis splines could adequately represent the autocorrelation data, certain details of the original speed distribution function were not being recovered from the autocorrelation data.

TABLE I

FIRST FOUR SPEED MOMENTS FOR SPEED DISTRIBUTION OF FIGS. 1 AND 2.

Distribution	χ_ν^2	$\bar{v}$	$<(v-\bar{v})^2>^{1/2}$	$<(v-\bar{v})^3>^{1/3}$	$<(v-\bar{v})^4>^{1/4}$
Fig. 1A (*a*)		20.3	11.0	8.5	13.5
(*b*)		18.5	10.8	9.5	14.1
Fig. 1B (*a*)	1.00 ± 0.04	18.5 ± 0.04	10.9 ± 0.19	9.3 ± 0.15	14.2 ± 0.20
(*b*)	1.00 ± 0.05	18.4 ± 0.06	11.0 ± 0.21	9.32 ± 0.16	13.8 ± 0.16
(*c*)	1.00 ± 0.05	18.3 ± 0.09	11.1 ± 0.26	9.2 ± 0.09	13.8 ± 0.18
(*d*)	1.01 ± 0.05	18.7 ± 0.04	10.5 ± 0.14	9.9 ± 0.19	13.8 ± 0.15
Fig. 2A (*a*)	1.00 ± 0.05	20.2 ± 0.06	11.2 ± 0.22	8.28 ± 0.09	13.7 ± 0.16
(*b*)	1.00 ± 0.05	18.4 ± 0.06	11.0 ± 0.21	9.32 ± 0.16	13.8 ± 0.16
Fig. 2B (*a*)	1.00 ± 0.04	20.2 ± 0.09	11.3 ± 0.28	8.01 ± 0.06	13.8 ± 0.20
(*b*)	1.00 ± 0.05	18.3 ± 0.09	11.1 ± 0.26	9.2 ± 0.09	13.9 ± 0.18
Fig. 2C (*a*)	1.00 ± 0.05	20.4 ± 0.04	10.9 ± 0.16	8.95 ± 0.20	13.6 ± 0.16
(*b*)	1.01 ± 0.05	18.7 ± 0.04	10.5 ± 0.14	9.9 ± 0.19	13.8 ± 0.15

χ_ν^2 is the average χ^2 per degree of freedom for the fits to each of the 10 sets of autocorrelation data used to determine each speed distribution. Data are in micrometers per second.

The quality of the fits indicated that this resulted from an insensitivity of the data to these details, rather than from any inability to fit the data.

KNOT SELECTION When only a few knots are used, the knot positions seem to determine the speed distribution functions that can be well represented. With this in mind, experiments were performed to evaluate the influence that knot replacement has upon the resultant fitted speed distribution. The autocorrelation functions generated from the speed distribution of Fig. 1 A (curve *b*) were fitted with several knot sets (Fig. 1 B). The differences seem significant, but Table I shows that for each of the fitted speed distributions the first four speed moments are nearly identical. The means of the fitted distributions differ from that of the assumed speed distribution by at most 1%. The autocorrelation data apparently do not contain enough information to specify accurately the fine structure of the speed distribution and yet are sensitive to the grosser characteristics reflected in the speed moments. Also, for any particular knot set, the shape of the resultant fitted distribution, as indicated by the error brackets, is quite restricted.

MEAN SPEED DISTRIBUTION To determine how successfully speed distributions could be resolved, two similar distributions (Fig. 1 A) whose mean speeds differed by roughly 10% (see Table I) were used to generate autocorrelation data. For each of four distinct knot sets, these functions were separately fitted; in each case, the two mean speeds calculated were discrete and closely approximated the means of the respective

TABLE II

SENSITIVITY TO SPEED DISTRIBUTION WIDTH

Generating function	Knot set	$\langle v \rangle$	$\langle (v - \bar{v})^2 \rangle^{1/2}$	$\langle (v - \bar{v})^3 \rangle^{1/3}$	χ^2_ν
(a)	—		10.79	0.03	
	1	20.2 ± 0.13	10.7 ± 0.26	5.6 ± 1.2	0.85 ± 0.03
	2	20.4 ± 0.07	10.3 ± 0.26	7.7 ± 0.4	0.85 ± 0.03
(b)	—	20.0	9.56	0.02	
	1	20.0 ± 0.13	9.75 ± .0.32	1.4 ± 2.3	0.85 ± 0.03
	2	20.2 ± 0.07	9.5 ± 0.18	5.4 ± 1.11	0.85 ± 0.03
(c)	—	20.0	9.10	−0.14	
	1	20.0 ± 0.13	9.39 ± 0.31	9.5 ± 2.1	0.85 ± 0.002
	2	20.1 ± 0.07	9.16 ± 0.19	3.6 ± 1.5	0.85 ± 0.01
(d)	—	20.0	7.51	−0.03	
	1	19.8 ± 0.10	8.17 ± 0.34	−0.67 ± 1.2	0.85 ± 0.03
	2	19.9 ± 0.06	8.15 ± 0.15	−0.22 ± 1.8	0.85 ± 0.03
(e)	—	20.0	4.06	−0.035	
	1	19.6 ± 0.05	7.8 ± 0.1	7.7 ± 1.3	0.95 ± 0.36
	2	19.5 ± 0.46	7.9 ± 0.02	−0.45 ± 0.9	1.04 ± 0.05

The first four speed moments are tabulated for both the assumed speed distributions (see Fig. 3) and for the distributions obtained by fitting the autocorrelation data generated with these assumed distributions. Two different knot sets, 1: (0, 5, 15, 25, 35, and 50 μm/s) and 2: (0, 13, 21, 30, 36, and 50 μm/s), were used to fit each set of autocorrelation data. The knot set used for each assumed speed distribution was (0, 10, 20, 30, and 40 μm/s).

distributions used to generate the data. In addition, for any knot set, the two fitted distributions were as easily distinguishable by simple inspection, as were the original speed distribution functions (see Fig. 2).

DISTRIBUTION WIDTH Data from speed distributions possessing identical means but different second moments were analyzed to ascertain the assay's sensitivity to variation in the width of the distribution. Except for the most sharply peaked distributions, the second moment of the distributions could be successfully recovered. Difficulties with narrow peaks occur because the spline function cannot satisfactorily represent them unless knots happen to be located at the peaks. Such good fortune is unlikely when the few knots are not specifically chosen for this purpose, an impossibility with experimental data. Because before an experiment the range of possible bacterial speeds can be only very roughly estimated, the problems of analysis of experi-

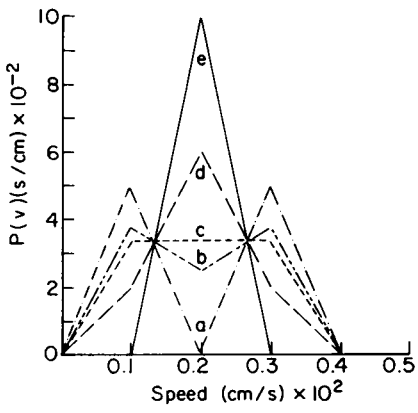

FIGURE 3

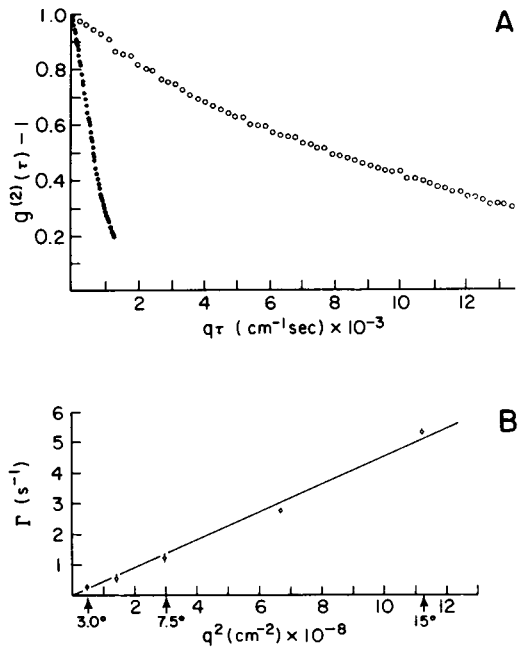

FIGURE 4

FIGURE 3 The five assumed speed distributions used to generate the synthetic data for Table II. The distributions have identical means but different widths.

FIGURE 4 Diffusion of nonmotile bacteria. (A) The autocorrelation function from a preparation of motile bacteria is shown before (•) and 5 min after (o) the addition of HCl. Data collection was at a scattering angle of 7.5° ($q = 1.73 \times 10^4$ cm^{-1}), at 30°C. The duration of each experiment was 100 s. (B) The decay constants for autocorrelation functions from nonmotile bacteria are plotted against the square of the scattering vector for several low scattering angles. Along the abscissa, several of the scattering angles are also indicated in degrees. Single exponential fits were used to fit $g^{(1)}(\tau)$ to $e^{-\Gamma\tau}$, where $\Gamma = D_T q^2$. The calculated diffusion constant was 4.3×10^{-9} cm/s^2. Here, the normalized intensity correlation function, $g^{(2)}(\tau)$, is plotted; before normalization, it commonly has an amplitude at $\tau = 0$ of about 1.8 times the theoretical background.

mental data were more accurately approximated by selecting for the assumed and fitted speed distributions different ranges of allowable speeds. This procedure had little effect on the values obtained for the mean and width of the calculated speed distributions.

Also apparent from these experiments (Table II and Fig. 3) is a consistent insensitivity to the skewness of the distribution, $<(v - \bar{v})^3>^{1/3}$. Because the quality of the fits can be good even when the skewnesses of the fitted and assumed speed distributions are different, it is unlikely that moments higher than the second moment of the bacterial speed distribution can be satisfactorily determined from experimental autocorrelation data.

INITIAL GUESSES The procedure employed to calculate the speed distribution successively improves, by iteration, an initial guess of the speed distribution. Generally, a uniform speed distribution was used as an initial guess. To establish that this guess did not significantly affect the final outcome of the fit, identical data were fitted using various initial guesses. It was found that with three basis splines the outcome was independent of the guess used; with four basis splines, it was very nearly so. As the number of basis splines was progressively increased, the calculated distribution became more and more influenced by the guess used; significantly, though, the values of the first two speed moments of the distributions were unaffected. In view of the earlier results, this behavior is easy to understand: as the number of knots is increased, more speed distributions that have equivalent autocorrelation functions can be represented: the parameters are no longer all independent. As the minimum in χ^2 space becomes less well defined, the speed distribution eventually selected by the fitting routine becomes more dependent upon the direction of approach. It is thus desirable not to use unnecessary parameters to describe the fitting function; this is done by progressively eliminating parameters until χ^2_ν increases significantly.

SUMMARY A reasonable procedure for fitting the experimental data can now be inferred: the same set of knots should be used for fitting any speed distributions that are to be compared, and the number of knots in this set should be minimal. Though the local structure of the fitted speed distribution is largely determined by the choice of knots, the general shape is not. Straightforward examination of the calculated speed distributions should allow an easy distinction to be made between sharply peaked and broad or bimodal distributions. Regardless of the knots selected, the first two moments of the speed distribution can be reproducibly and accurately obtained from autocorrelation data.

Experimental Data

The extraction of useful information about bacterial speed distributions from actual experimental data is substantially more difficult than the analysis of computer-generated data. With real data, our analytic model is only an approximation, serving to simplify the problem and to allow the calculation of parameters of interest. The danger that the model of bacterial movement might be insufficiently accurate for faithful representation of those qualities under study, thus causing a faulty interpretation

of the data, makes it essential to examine thoroughly the characteristics of the collected data, and also to obtain some independent verification of the estimates obtained by the procedure.

To estimate the relative rates of motion during different periods of measurement, comparisons were made either between the autocorrelation functions themselves, or, alternatively, between the time for the autocorrelation functions to decay to one-half amplitude, $t_{1/2}$. Unfortunately, such comparisons can prove misleading when differently shaped autocorrelation functions with similar overall rates of decay are compared, so that a more quantitative method, the examination of the parameters obtained by spline analysis of the bacterial speed distributions, was often required.

CONVECTION Motile bacteria ordinarily have translational speeds averaging about 20–30 μm/s. Since autocorrelation data obtained from particles translating at this rate could be distorted by slight thermal convection, great care was taken to eliminate it (18). In Fig. 4 A, autocorrelation functions from motile and nonmotile bacteria are shown. The diffusion constant of the nonmotile bacteria was determined by plotting the decay constant of the exponentially decaying autocorrelation function against q^2 (7). The linearity of Fig. 4 B demonstrates the absence of significant con-

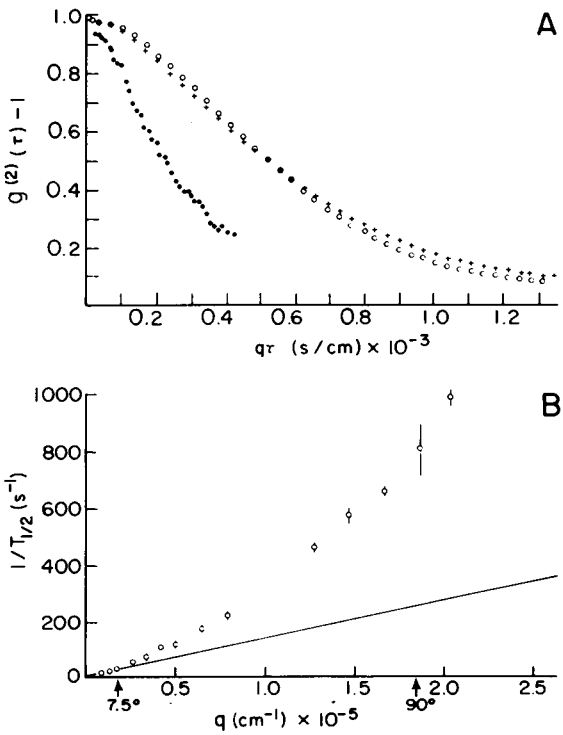

FIGURE 5 $q\tau$ scaling. (A) The experimental autocorrelation functions of motile bacteria are plotted for scattering angles of 3.7°(○), 7.5°(+), and 90°(●). The approximate $q\tau$ scaling at the low angles is to be contrasted with the more rapid decay at 90°. (B) Data from motile bacteria is plotted for a more complete set of scattering angles. The bacteria were suspended in NB at 30°C.

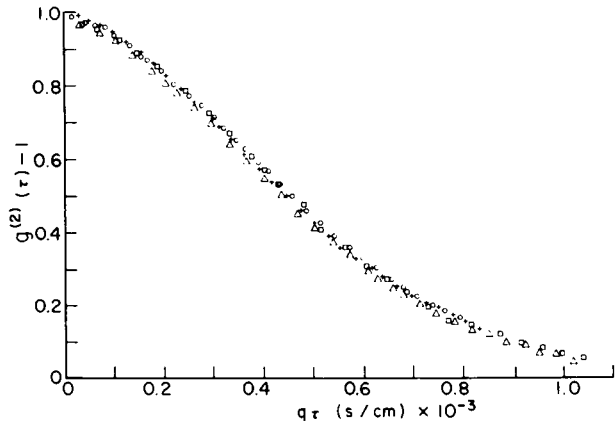

FIGURE 6 Low-angle $q\tau$ scaling. Autocorrelation functions taken at 7.5°(+), 6°(△), 5°(○), and 3°(□) are plotted. Each plotted function is the average of three successive runs of 100 s duration. All of the data was taken over a period of 30 min on the same sample of *Salmonella* in NB at 30°C.

vection. This detection of slow diffusion indicates that convection is not contaminating the faster decaying autocorrelation data from motile bacteria.

$q\tau$ SCALING Bacteria that are not rotating and are actively translating, rapidly relative to diffusion, have autocorrelation functions at different scattering angles that superimpose when plotted against $q\tau$ (16). This is called "$q\tau$ scaling" and, when it obtains, the plot of $1/t_{1/2}$ versus q is linear. At high scattering angles, rotational movement contributes to the autocorrelation functions and increases their decay rate beyond this $q\tau$ scaling level (Fig. 5 A). The rotational contribution progressively increases as the scattering angle is raised and gradually expands the deviation from linearity in Fig. 5 B. Nevertheless, at low scattering angles, $q\tau$ scaling obtains (Fig. 6) and the calculated speed distributions are nearly independent of angle.

These results confirm the scaling behavior previously predicted (16); that the speed parameters calculated from the low-angle data accurately reflect the actual bacterial speed distributions is shown by the cinematographic experiments described below.

CINEMATOGRAPHY Cinematographic and PCS measurements were performed simultaneously on identical aliquots of a single bacterial preparation and the results obtained from the two techniques were in good agreement. The cinematographic analysis, however, did not reveal any bacteria moving more rapidly than 60 μm/s, while PCS indicated a large primary peak centered at 22 μm/s, with an area of about 92% of the distribution, and a small secondary peak located at approximately 100 μm/s. The major peak of the speed distribution obtained by light scattering quite accurately reflects the actual speeds of the actively translating bacteria (Fig. 7). The significance of the small secondary peak will be examined later; apparently, it is not a direct result of bacterial translation.

DETAILED STRUCTURE OF THE SPEED DISTRIBUTION FUNCTION The speed distributions from bacterial preparations usually contain three distinct components: a

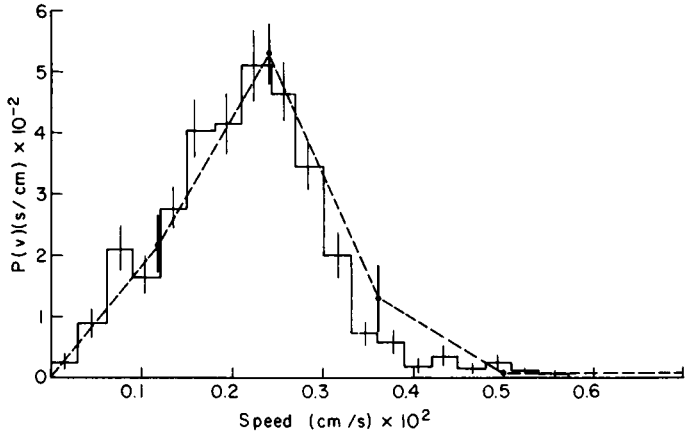

FIGURE 7 The normalized speed distribution obtained by tracking 500 bacteria (bar graph) is compared with the speed distribution obtained by PCS (●). For the bar graph, each error estimate indicates the square root of the number of bacteria at that speed; for the light scattering results, it indicates the standard deviation of the mean for determinations from five autocorrelation functions of 100 s duration. For the cinematographic distribution $\bar{v}$ = 21.4 μm/s; for the light scattering distribution, $\bar{v}$ = 22.5 ± 0.9 μm/s and β = 0.11 ± 0.04. $\bar{v}$ was calculated without including nonmotile bacteria or the high-speed peak of 8.4 ± 0.6%. Knots were evenly spaced at 12, 24, and 36 μm/s. Autocorrelation data was from a 7.5° scattering angle. *Salmonella* were suspended in NB at 24°C for PCS and at 23°C for cinematography.

primary peak between 0 and 50 μm/s, a small secondary peak at high speeds (~100 μm/s), and a nonmotile fraction of variable size.

High-speed peak. The location of the high-speed peak could be altered by changing the positions of the high-speed knots while keeping the other knots stationary. From changes in the magnitude of χ^2_ν for different fits, it was determined that suc-

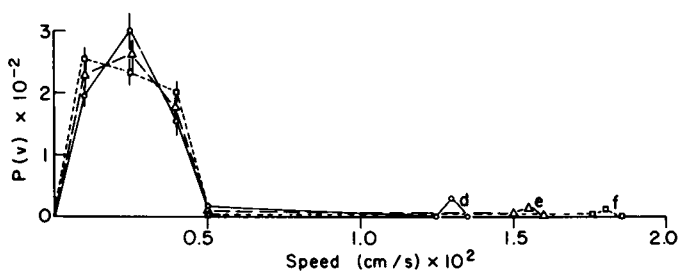

FIGURE 8 High-speed peak. Spline fits with different allowed high-speed peaks were made to the same experimental autocorrelation functions. The data, taken at 30°C, were from a scattering angle of 7.5°. The error bars, in each case, represent the standard deviation of the mean for five sets of data. In all cases the lower knots were: (0, 0.001, 0.0025, 0.004, 0.005 cm/s). The higher knot positions were as follows: *d*: (0.0125, 0.0130, 0.0135); *e*: (0.0150, 0.0155, .0160), *f*: (0.0175, 0.0180, 0.0185). For the three fits respectively, β was: 10.5% ± 1.5, 9.5% ± 2.0, 9.5% ± 1.8, $\bar{v}$ was: 21.0 ± 1.2, 21.2 ± 1.0, 21.1 ± 1.3 μm/s, and the fraction of the distribution located above 60 μm/s was: 7.5% ± 0.4, 7.2% ± 0.2, 6.4% ± 0.3.

cessful fitting of the autocorrelation data requires a peak at or above 90 μ/s. The exact position of this peak has little influence on the estimate of either the nonmotile fraction, β, or the mean speed of the distribution (Fig. 8). Though the area of the peak itself gradually diminishes as it is displaced to higher speeds, the total area located at speeds greater than 60 μm/s remains relatively constant (18).

The source of this high-speed component is not understood; the cinematographic results strongly suggest that it is not directly related to the translational movement of the bacteria. The secondary peak appeared in all fits and amounted to between 4% and 8% of the area of the speed distribution: its size was essentially independent of scattering angle (18). The peak might be attributable to light scattered by the flagella of the bacteria. Fortunately, it does not seem to interfere with the precise determination of translational speed parameters. Although the significance of this peak might prove to be very interesting, further investigation of it has been deferred in favor of an application of the analysis in its present state to the measurement of bacterial motility under a variety of interesting conditions.

Nonmotile fraction. The "nonmotile" fraction, β, (17) actually represents very slowly translating bacteria as well as nonmotile ones, and hence is misnamed. It ordinarily constitutes between 5% and 30% of the bacterial population. It could be more appropriately labeled the "low-speed fraction," and can be adequately represented by either the term β or by a very low-speed spike; the choice of representation has little effect on either the size of the fraction or the accuracy of the data fit (18).

It is felt that this fraction, to a large extent, consists of the "twiddling" bacteria described by Berg (2). Such bacteria exhibit a rather jerky uncoordinated motion and thus have a comparatively slow rate of net translation. A close relationship might exist between β and the average proportion of time a bacterium spends undergoing

TABLE III

THE MEASURED $\bar{v}$ OF BACTERIA AND β (NONMOTILE FRACTION) FOR MIXTURES OF MOTILE BACTERIA AND 1.1 μm LATEX SPHERES

Motile fraction		$\bar{v}$	β
		μm/s	
0		-0.1 ± 0.4	1.01 ± 0.02
1.0		22.5 ± 1	0.18 ± 0.07
0.75 ± 0.02	calc.	17.1 ± 2	0.38 ± 0.06
	expt.	18.1 ± 0.3	0.35 ± 0.01
0.62 ± 0.02	calc.	14.0 ± 2	0.49 ± 0.08
	expt.	13.2 ± 0.4	0.475 ± 0.02

The expected values of $\bar{v}$ and β were calculated on the basis of the mixture composition (motile fraction) and the parameters of the pure preparations. Measurements were at a 7.5° scattering angle, at 30°C. Each tabulated experimental value represents the average from three autocorrelation functions.

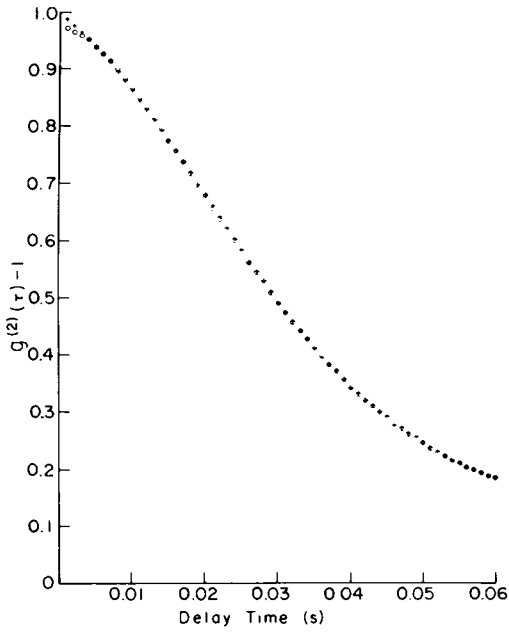

FIGURE 9 Fitted data. The average of 10 normalized autocorrelation functions, each of 100 s duration, was fitted using a spline fit containing 7 parameters, including β. The experimental (+) and fitted (o) autocorrelation functions are compared. Bacteria were suspended in CHE at 30°C. The scattering angle was 7.5°.

directional changes. Under normal experimental conditions, scattered light is always being collected from 1,000 or more bacteria, and this average would closely approximate the fraction of bacteria which exhibit this motion at any time. Between different bacterial samples, β tends to vary much more than do other parameters of the speed distribution, such as the mean speed. Microscopic observation of different cultures also indicates that the frequency of directional changes of bacteria is quite variable.

To clarify the interpretation of the term β, data were collected from mixtures of pre-

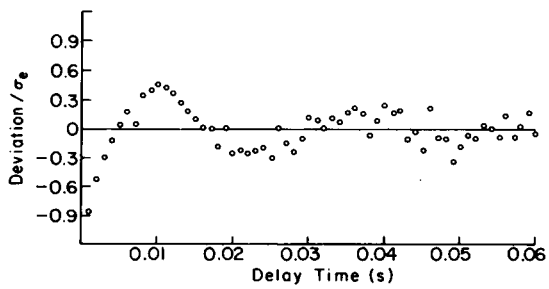

FIGURE 10 Residuals. The residuals of the fit to the data of Fig. 7 are plotted. The standard deviation of the mean, σ_e, at each point of the autocorrelation function was calculated from the variation between the ten individual data sets. $\chi^2_\nu = 0.067$.

determined quantities of active bacteria and polystyrene latex spheres of diameter 1.1 μm. It was found that the polystyrene component could be successfully identified (Table III) (18).

NUMBER OF FITTING PARAMETERS Experimental autocorrelation data were usually fitted-using seven parameters: four basis splines to represent the translational speed distribution, two basis splines to allow a separate secondary peak, and one basis spline (or the term β) to represent the nonmotile fraction. When the number of fitting parameters used was reduced below seven, the quality of the fits, as measured by χ^2_ν, began to suffer; when the number of parameters was raised much above this, the uniqueness of the fits was diminished.

DATA PRECISION AND GOODNESS OF FIT Despite slight variations in the overall shape of the autocorrelation functions from experiment to experiment, individual autocorrelation functions were quite smooth as a result of the correlations between the values of the function at adjacent delay times. Slight contributions to the scattered field from sources other than bacteria, for example, dust, could account for such minor variation without substantially degrading the quality of the data fits. Such contribu-

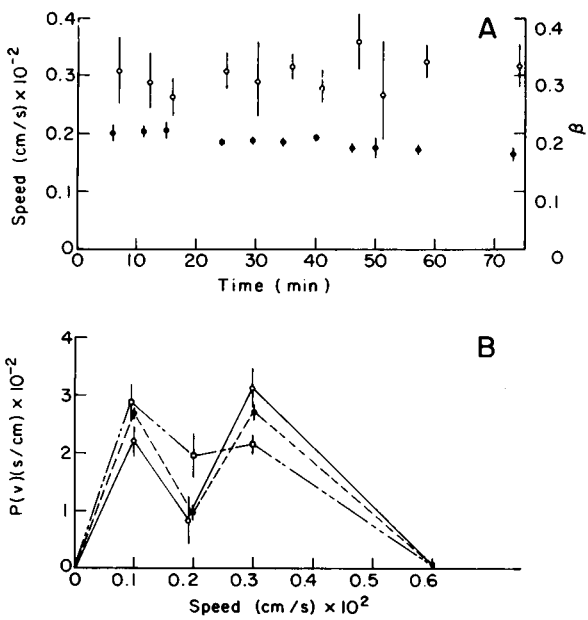

FIGURE 11 Sample stability. (A) The stability of a culture at low concentration ($\sim 2 \times 10^7$ cells/ml) was examined. The mean of the speed distribution of all bacteria and β are plotted against the time that the bacteria have been in the light-scattering cuvette. At time 0, the bacteria were added from a concentrated NB culture at 4°C to a cuvette containing CHE buffer at 30°C. Each average speed (•) and standard deviation of the mean was calculated from three or four successive 100-s experiments. The nonmotile fraction (○) is also plotted. The data was collected at a scattering angle of 7.5°. (B) The speed distributions obtained at the times of 6 min (○), 35 min (•), and 70 min (□). The initial bimodal nature of the translational speed peak seems to diminish slowly with time.

tions, though increasing the variation in the data points, did not introduce into the autocorrelation functions components that could not be fitted by the bacterial model (18); thus, when the error in the individual data points was estimated directly from a consideration of successive "identical" experiments, χ^2_ν for the data fits was much less than 1.

When a single experiment was fitted, the residuals appeared fairly evenly distributed about zero; when many experiments were averaged and then fitted (Fig. 9), a systematic deviation in the fit was revealed in the residuals (Fig. 10). The presented data illustrate this feature of the fit clearly; in some cases the effect was reduced in magnitude, but it was never entirely absent. This consistent deviation between the experimental data and the fitted autocorrelation function reveals the inability of the theoretical model to explain fully the fine structure in the autocorrelation data. As this deviation is most marked at very short delay times, it is probable that it results from the same causes that necessitate a high-speed component in the speed distribution. Since the component of the autocorrelation function giving rise to the high-speed peak is not directly related to bacterial translation, it is represented inappropriately by a "high-speed peak," and so the imperfect duplication of the early decay of the autocorrelation function is not surprising.

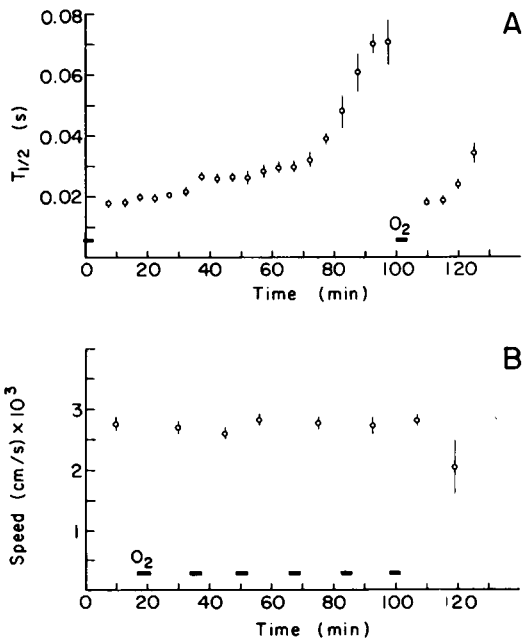

FIGURE 12 Anaerobiosis at high cell concentrations. (A) $t_{1/2}$ of the decay of the intensity autocorrelation is plotted vs. time. The bacteria were suspended in NB at 30°C at an initial concentration of 6.0×10^8 cells/ml. The decrease in activity that accompanied O_2 depletion was restored by oxygenation (▬). (B) The mean speed, including β, of a concentrated bacterial culture in NB at 30°C was measured over 2 hr. An active culture was maintained by oxygenating the sample periodically. Data was collected at a scattering angle of 7.5°.

SAMPLE STABILITY To compare the motility of bacteria under a variety of conditions, it is necessary to have reproducible samples that will maintain an approximately constant level of motility for a sufficient period of time. This has been achieved. When an active culture was cooled to 4°C and stored at that temperature, aliquots taken over a period of several days and warmed to 30°C for light scattering measurements were found to exhibit equivalent ($\pm 10\%$) mean speeds. In addition, the individual samples warmed to 30°C maintained a fairly stable motility for more than 1 h (Fig. 11). When suspended at low concentrations ($\leq 2 \times 10^7$ cells/ml), cells did not require oxygenation to maintain their activity, but at higher concentrations they rapidly metabolized the oxygen in the medium and became sluggish. This loss of activity could be reversed by oxygenating the medium (see Fig. 12 A). Even at high concentrations ($\sim 6.0 \times 10^8$ cells/ml), though, suspensions could be maintained at a constant level of motility by periodic oxygenation of the medium (Fig. 12 B). In CHE, the level of bacterial motility seemed to be nearly independent of the concentration at which the bacteria were suspended (18). In NB suspensions, the bacteria would grow and change the composition of their environment, which would in turn alter their activity. The changes depended both on the density of the bacterial suspension and on how long the bacteria had been growing in the suspension.

CONCLUSION

These experiments establish the practicability of using PCS as a rapid and accurate assay of bacterial translational movement. Though some details of the experimental autocorrelation functions are still not understood and warrant further study, many aspects of the motile behavior of bacteria can now, for the first time, be quite easily examined. To be able to easily alter the environment of bacteria and quickly measure their motility without significantly perturbing them suggests many exciting experiments. It is hoped that interesting results will soon be forthcoming from some of the experiments now being planned in this laboratory.

Much of the work contained in this manuscript was submitted as partial fulfillment of the requirements for the degree of Doctor of Philosophy at The Johns Hopkins University. It is a pleasure to acknowledge the valuable advice and support of Professor F. D. Carlson.

This work was supported by funds from U.S. Public Health Service Training Grant 5T01 GM00716, Grant AM12803 to F. D. Carlson, and Postdoctoral Fellowship 1-F32-GM06216-01 to G. B. Stock.

Received for publication 19 November 1977.

REFERENCES

1. BANK, G., D. W. SCHAEFER, and S. S. ALPERT. 1975. Light-scattering study of the temperature dependence of *Escherichia coli* motility. *Biophys. J.* **15**:253–261.
2. BERG, H. C. 1975. Review article. Bacterial behaviour. *Nature (Lond.).* **254**:389–392.
3. BERNE, B. J., and R. NOSSAL. 1974. Inelastic light scattering by large structural particles. *Biophys. J.* **14**:865–880.
4. BOON, J. P., R. NOSSAL, and S.-H. CHEN. 1974. Light scattering spectrum due to wiggling motions of bacteria. *Biophys. J.* **14**:847–864.

5. CARLSON, F. D., R. BONNER, and A. FRASER. 1972. Intensity fluctuation autocorrelation studies of resting and contracting frog sartorius muscle. *Cold Spring Harbor Symp. Quant. Biol.* **37**:389–396.
6. CHEN, S.-H., M. HOLTZ, and P. TARTAGLIA. 1977. Quasi-elastic scattering from structured particles. *Appl. Opt.* **16**:187–194.
7. CUMMINS, H. Z., F. D. CARLSON, T. J. HERBERT, and G. WOODS. 1969. Translational and rotational diffusion constants of tobacco mosaic virus from Rayleigh linewidths. *Biophys. J.* **9**:518–546.
8. CUMMINS, H. Z. 1976. Intensity fluctuation spectroscopy of motile microorganisms. *In* Photon Correlation Spectroscopy and Velocimetry. H. Z. CUMMINS and E. R. PIKE, editors. Plenum Publishing Corp., New York. 200–226.
9. GOLL, J., and G. B. STOCK. 1977. Determination by photon correlation spectroscopy of particle size distributions in liquid vesicle suspensions. *Biophys. J.* **19**:250–256.
10. NOSSAL, R., S.-H. CHEN, and C. C. LAI. 1971. Use of laser scattering for quantitative determinations of bacterial motility. *Opt. Commun.* **4**:35–39.
11. NOSSAL, R., and S.-H. CHEN. 1972*a*. Light scattering from motile bacteria. *J. Phys. (Paris).* **33C1**:171–176.
12. NOSSAL, R., and S.-H. CHEN. 1972*b*. Laser measurements of chemotactic response of bacteria. *Opt. Commun.* **5**:117–122.
13. SCHAEFER, D. W. 1973. Dynamics of number fluctuations: motile microorganisms. *Science* (Wash. D.C.). **180**:1293–1295.
14. SCHAEFER, D. W., G. BANKS, and S. S. ALPERT. 1974. Intensity fluctuation spectroscopy of motile micro-organisms. *Nature (Lond.).* **248**:162–164.
15. SCHAEFER, D. W. 1975. *In* Laser Applications to Optics and Spectroscopy. S. F. JACOBS, M. O. SCULLY, M. SARGENT, and J. F. SCOTT, editors. Addison-Wesley Co. Reading, Mass.
16. STOCK, G. B., and F. D. CARLSON. 1974. Photo autocorrelation spectra of wobbling and translating bacteria. *In* Symposium on Swimming and Flying in Nature. T. Y-T WU, C. J. BROKAW, and C. BRENEN, editors. Plenum Publishing Corp., New York. 57–68.
17. STOCK, G. B. 1976. Application of splines to the calculation of bacterial swimming speed distributions. *Biophys. J.* **16**:535–540.
18. STOCK, G. B. 1977. Photon correlation spectroscopy. An assay of bacterial motility. Ph.D. Thesis, Johns Hopkins University. Baltimore, Md. University Microfilms, Ann Arbor, Mich.